SANDIA REPORT
SAND2022-7719
Printed June 2022
UUR

Sandia National Laboratories

Thermochemical characterization of intumescent materials and their application in FEM models using Aria

Sean M. Babiniec, Emilee L. Reinholz, Eric N. Coker, Marin E. Larsen

Prepared by
Sandia National Laboratories
Albuquerque, New Mexico
87185 and Livermore,
California 94550

Issued by Sandia National Laboratories, operated for the United States Department of Energy by National Technology & Engineering Solutions of Sandia, LLC.

Available to DOE and DOE contractors from
U.S. Department of Energy
Office of Scientific and Technical Information
P.O. Box 62
Oak Ridge, TN 37831

Telephone: (865) 576-8401
Facsimile: (865) 576-5728
E-Mail: reports@osti.gov
Online ordering: http://www.osti.gov/scitech

Available to the public from
U.S. Department of Commerce
National Technical Information Service
5301 Shawnee Rd
Alexandria, VA 22312

Telephone: (800) 553-6847
Facsimile: (703) 605-6900
E-Mail: orders@ntis.gov
Online order: https://classic.ntis.gov/help/order-methods/

ABSTRACT

Intumescent materials are in wide use as protective coatings in fire protection or thermal management applications. These materials undergo chemical reactions occurring from approximately 300°C to 900°C, which outgas and expand the material, providing an appreciable increase in insulative performance. However, the complicated chemical mechanisms and large changes in materials properties complicate the incorporation of these materials into predictive thermal models. This document serves to outline the thermochemical characterization of select intumescent materials, the extraction of relevant parameters, and the incorporation of these parameters into the ChemEQ reaction model implemented in Aria. This work was performed in 2016 and documented in a draft SAND report in March 2017. In 2022, the draft SAND report was discovered and put through R&A.

ACKNOWLEDGEMENTS

This work was performed in 2016 and documented in a draft SAND report in March 2017. In 2022, the draft SAND report was discovered and put through R&A by Karen Son.

CONTENTS

LIST OF FIGURES

LIST OF TABLES

This page left blank

ACRONYMS AND TERMS

Acronym/Term	Definition
DSC	differential scanning calorimetry
DTA	differential thermal analysis
FE	finite element
IM	intumescent material
MS	mass spectrometry
TGA	thermogravimetric analysis

1. INTRODUCTION

The present investigation is motivated by a requirement to develop a thermally-resistant wall design with an intumescent passive fire protection coating. Such coatings are frequently used to maintain structural integrity of steel [1]–[5], aluminum [6], laminates [7], and glass fiber-reinforced epoxy composite [8] substrates to protect buildings, ships [6], liquefied petroleum gas tanks [9], and other industrial or petrochemical environments both on- and offshore in the event of hydrocarbon pool fires or jet fire impingement [10]. Tests such as UL-1709 and NORSOK M-501 provide thermal response, physical endurance, and weathering resistance performance data [10]. Yet, even with these stringent testing standards, evaluation of specific designs and applications would benefit largely from improved modeling of intumescent materials (IMs). Many IM models exist; most are one-dimensional mathematical models that include kinetics, gas evolution and entrapment, and/or IM expansion[1]–[4], [11]. To the best of our knowledge, only Asaro et al. [6] and Landucci et al. [9] have developed finite element (FE) IM models. Asaro [6] applied simplified kinetics for a single-stage reaction, where other authors have shown that IMs experience oxidative degradation in three reactions [3], [12]. Landucci et al. [9] used constant thickness and properties with no inclusion of thermochemical changes in their FE model. We strive to better characterize the thermochemical behavior of an IM using a finite element model. Like Di Blasi et al. [4] and Branca et al. [12], we apply Arrhenius kinetics for a three-stage oxidative degradation process. The predicted reaction extent is then used to indicate the extent of transition of thermal transport properties from the virgin material to the fully reacted material.

Our objective is to limit the temperature excursion on the cooler side of a wall exposed to fire. The candidate design includes an IM layer that will decompose and expand when exposed to an abnormal operating environment of fire, creating a stable char layer. If the fire conditions continue well past decomposition, the thermal resistance of a stable char may be more important than thermal response delay attributed to the decomposition reactions. Therefore, there is a need for a better model to predict the thermal performance of the intumescing layer. A model addressing the thermal response of a system must correctly predict rates of chemical decomposition and transport through the decomposition products for varied heating rates and maximum temperatures. This report documents the development of the chemical parameters of such a model.

Two IM materials were chosen as possible candidates for fire protection coatings. Each of these materials undergo significant expansion during reaction, providing an interesting and beneficial change in thermal properties. The following describes thermal experiments performed on very small samples of the IM, as well as the extraction of kinetic and thermodynamic parameters for chemical reaction rate predictions and heats of reactions, respectively. Additionally, the extracted parameters are incorporated into a ChemEQ materials definition in Aria, allowing the simulation of IM behavior in FE models.

1.1. Materials Candidates

The two IM materials of interest are Technical Fibre Products Technofire® 67152B and Carboline Pyroclad® X1. Each of these materials exhibit over a ten times expansion after fully reacting. Although much of the composition is proprietary, there are a few notable differences in the two materials. Technofire® is supplied as a sheet with an adhesive backing, making the application process consistent and convenient. It also contains an inert glass fiber which is intended to lend strength to the material as it reacts. Conversly, Pyroclad® X1 is supplied as a 2-part mixture, and must be properly prepared [13], [14] to maintain homogeneity and consistent performance.

This page left blank

2. CHARACTERIZATION METHODS

2.1. Thermal Analyses

Thermogravimetric analysis (TGA), differential thermal analysis (DTA), and mass spectrometry (MS) provided insight to the thermal decomposition of the intumescent material. A Netzsch STA 409 CD thermogravimetric/differential thermal analyzer (Netzsch, Selb, Germany) generated TGA/DTA data under a 100 ml min-1 flow of either argon (UHP grade, Matheson, Basking Ridge, NJ) or air (ultra-zero grade, Matheson) between 25 and 1100 °C. A Hiden HPR-20 mass spectrometer (Hiden, Warrington, England) sampled the gas exiting the TGA/DTA furnace via a 2m heated capillary inlet. Specimens of intumescing material were cut from a sheet using a razor blade and had dimensions of approx. 10 mm x 10 mm x 0.5 mm (mass ca. 160 mg). Each test specimen was placed in the bottom of a 5 ml alumina cup in the TGA/DTA instrument. Once sample mass and gas flow had reached steady state at 25°C, the TGA furnace was heated at a rate of 20, 30, 40, or 50 °C min-1 for Technofire®, and 3, 6, 12, and 20 °C min-1 for Pyroclad®. Each set of samples was heated to 1100 °C (1200°C in the case of 50 °C min-1 ramp). The higher ramp rates used for Technofire® were chosen to be more indicative of the heating rates observed in a fire. However, these rates were significantly lower in Pyroclad® in an effort to better de-convolve the separate reaction steps during char formation. Baseline correction runs were conducted by running each temperature/gas profile with an empty specimen cup; the baseline TGA data was then subtracted from the specimen TGA data to remove artefacts due to buoyancy changes. An S-type thermocouple in contact with the bottom of the alumina specimen cup monitored the temperature of the specimen, which was used in data analysis (as opposed to the furnace temperature).

This page left blank

3. RESULTS AND DISCUSSION

3.1. Thermal Analyses

3.1.1. Technofire® 67152B

TGA data collected for both Technofire® and Pyroclad® is illustrated in Figure 1. Comparing Figure 1 a) and c), it is immediately evident that the Pyroclad® intumescent experiences a larger weight percent loss due to thermal decomposition in argon; approximately 70% as compared to the 50% observed in the Technofire® experiments. However, the fraction of mass lost is nearly equal in the non-inert air environment. Mass spectroscopy data for Technofire® presented in Figure 3, suggests that the presence of air causes combustion of organics present in the material, as evidenced by the increase in both water but also most notably carbon dioxide formation. The mass loss in argon is most likely explained by dehydration, decomposition, and minor combustion of organics occurring around 400°C, where the air environment experiences full combustion due to surplus availability of oxygen reactant. The TGA patterns in Figure 1 a) and b), as well as the mass derivative in Figure 2, (Technofire®) suggest that three separate reaction mechanisms are occurring, and kinetic parameters for each of these three reactions are extracted (presented subsequently). The DSC presented in Figure 4 is indicative of broad, exothermic reaction behavior.

3.1.2. Pyroclad® X1

Pyroclad® differs from Technofire® insofar as the total mass lost displayed in Figure 1 c) and d) does not substantially differ between argon and air exposure. Mass spectrometry data observed in Figure 5 illustrates a qualitatively large amount of water production at relatively low temperatures of 200-400 °C, decoupled from other combustion products such as carbon dioxide. This indicates that there is a large hydrated species in the product, and these species thermally evolves hydrogen regardless of the oxygen partial pressure in the gas environment, as would be expected. This assertion is further supported by the materials safety data sheet (MSDS), which lists a large constituent (25-40%) of part A of the mixture is boric acid (H_3BO_3). Boric acid has been shown to significantly dehydrate at temperatures above 100°C, producing gaseous water [15]. Supporting differential scanning calorimetry (DSC) data is offered in Figure 6, which shows entirely endothermic reactions, consistent with dehydration and species dissociation. The black line in this figure is for a pre-reacted sample and is not of interest. It is evident in Figure 1 c) and d) that there is an accelerated mass loss in air at approximately 500°C likely due to combustion, which is corroborated in Figure 5 by the formation of carbon dioxide along with water at this temperature. Since the primary environment of this application will likely be air, focus is reserved for such cases. By observation of the TGA data (Figure 1 c) and d), Figure 2), it was determined that four primary reactions are identifiable, with the first being endothermic dehydration. In an effort to quantify reaction enthalpies, a sample was dried to remove the endotherms associated with dehydration and was analyzed by DSC. This data is presented in Figure 7 (blue line), which shows five total reaction events, although the second is very minor and is likely associated with the same mass event, and the last occurs very near the end of the experiment where no mass change is observed. The events generally align with visible changes in mass and can be integrated to provide estimates of reaction energies for each of the three exothermic reaction events. The endotherm from dehydration is estimated using the enthalpy of evaporation for water (2257e3 J/kg) and a nominal mass change of 10% observed in the TGA data for the first event. These estimates are provided in Table 1.

Table 1: Reaction energies for Pyroclad® X1

Reaction	Likely Event Description	Energy (J/kg) (exo-positive)	Method
1	Evaporation	-225.7E3	Calculated water evaporation
2	Decomposition	236.5E3	DSC
3	Combustion	2206E3	DSC
4	Combustion	1161E3	DSC

It should be noted that the reaction energies provided in Table 1 must be scaled to account for 1) the current mass of the material (instead of the initial mass as reported by the DSC software), and 2) the fraction of energy retained in the solid. Because the DSC is reported as energy per unit of initial mass, the measurement must be scaled by the change in mass (Δm_i) during each reaction. In scaling these energies, the values of Δm_i used are those resulting from the kinetics model explained in the next section (Section 3.2). The decision to use the modeled mass fractions instead of the mass fractions from the raw data arises from the desire for the model to be self-consistent; the modeled energy is consistent with the modeled mass loss.

Furthermore, it is realized that the reaction releases a gas which convects away from the solid, carrying with it some amount of energy. This means that the entire energy of the reaction is not applied to the solid, but some fraction remains in the solid, and the rest is lost in the environment through the release of the gas species. An initial assumption is made that the evolved gas is isothermal with the solid. Therefore, the energy fraction applied to the solid is the ratio of the specific heat of the solid to the total specific heat, or:

$$\Delta H_{\text{frac,solid}} = \frac{\Delta\overline{m}\cdot c_{p,\text{gas}}}{\Delta\overline{m}\cdot c_{p,\text{gas}} + \left(1-\Delta\overline{m}\right)c_{p,\text{solid}}} \quad 1$$

where $\Delta H_{frac,solid}$ is the fraction of the enthalpy applied to the solid, $\Delta\overline{m}$ is the mass change in a specific reaction normalized by the initial mass of that reaction, which describes the fraction of mass lost as gas during the reaction of interest. The specific heats of the solid was measured as a function of temperature, and the specific heat of the gas was estimated as a function of temperature for a mixture of water and carbon dioxide; the ratio of which was estimated using the mass spectroscopy data in Figure 3 for each reaction. The scaling factors and resulting enthalpy applied to the solid for each reaction is summarized in Table 2. The values are also reported in volumetric units (multiplied by an initial density of 1128.0 kg-m^{-3}) to avoid further scaling in Aria as the mass in each cell changes (volume is treated as constant).

Table 2: Scaling factors and reaction enthalpies applied to the solid

Reaction	Mass Change Scaling Factor	Solid Fraction Scaling Factor	Enthalpy applied to solid (J/m^3)
1	0.156	0.62	-2.54E8
2	0.338	0.40	3.61E7
3	0.114	0.62	1.76E8
4	0.083	0.81	8.80E7

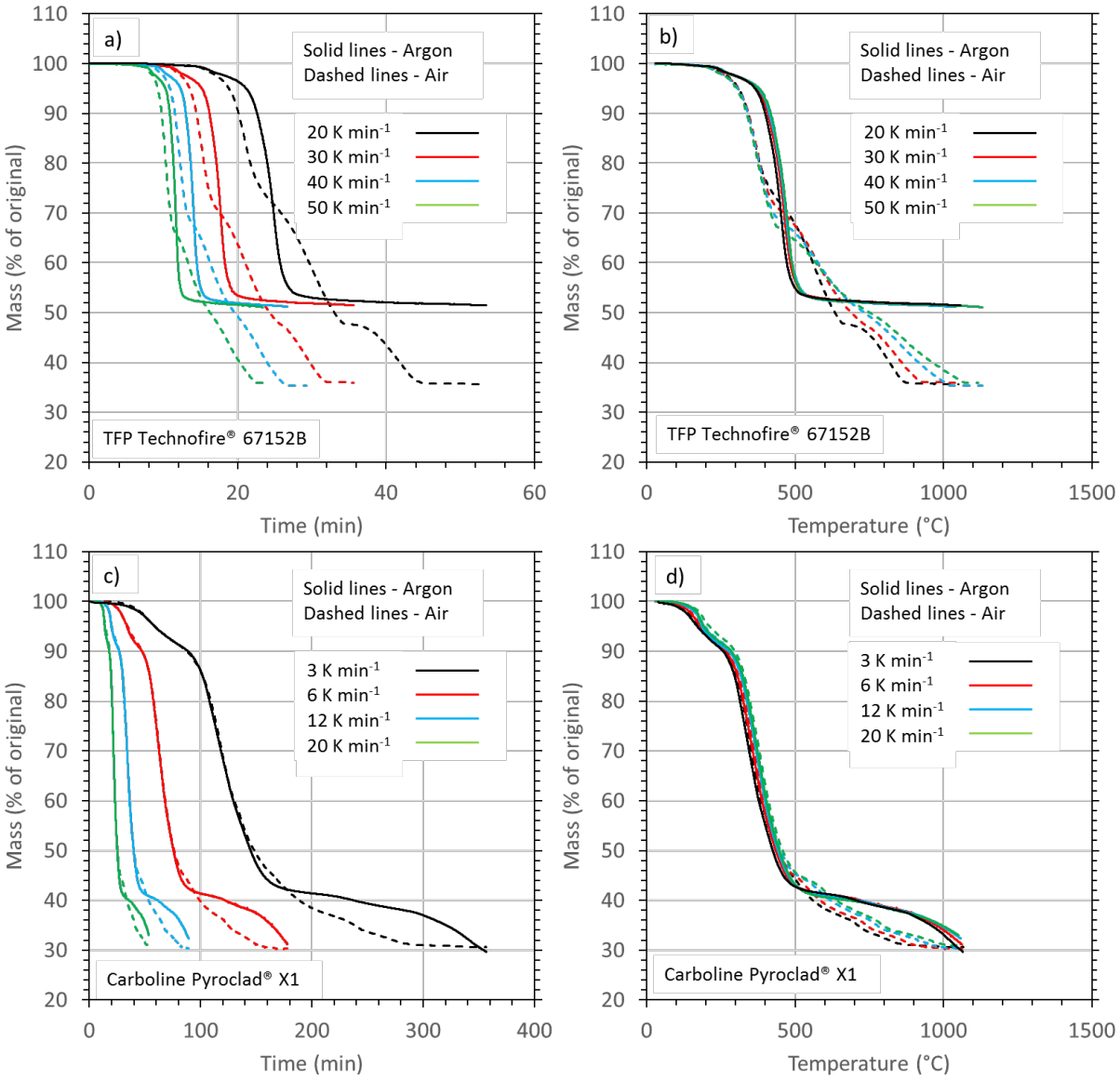

Figure 1. Comparison of TGA response of Technofire® (a & b) and Pyroclad® (c & d) IM. Mass percent is displayed versus time (a & c) and temperature (b & d).

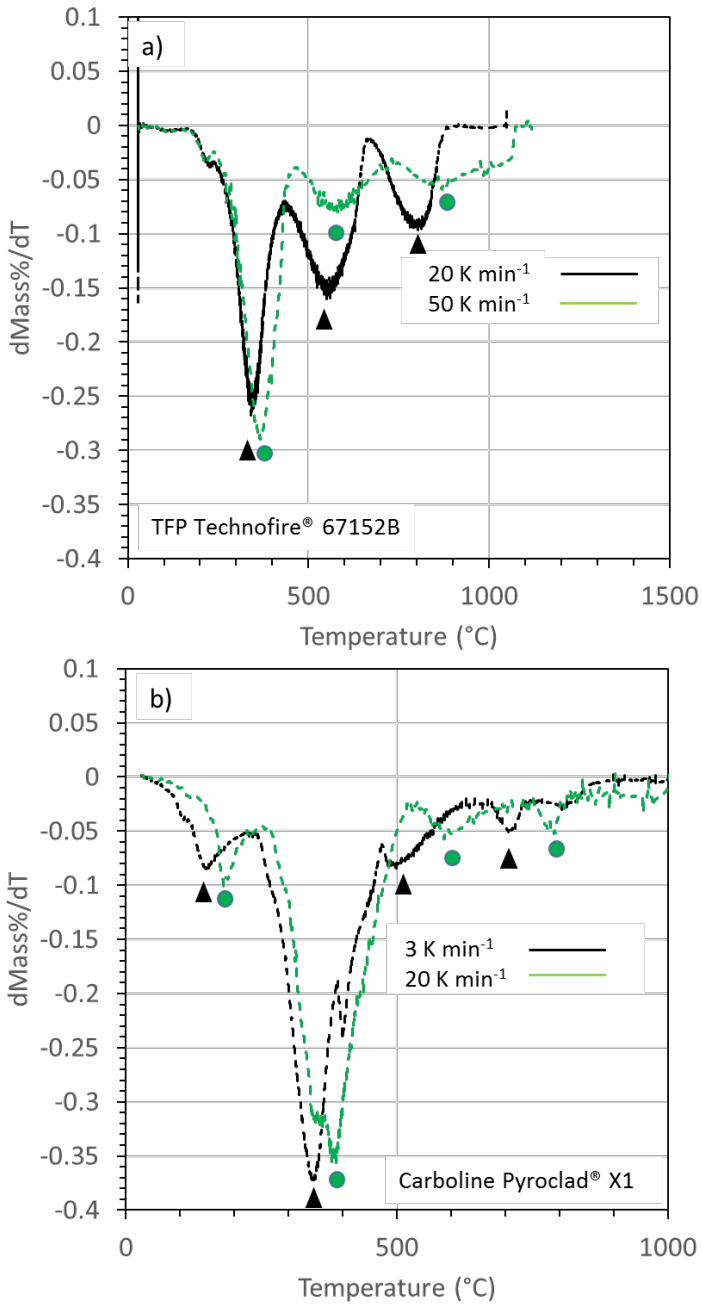

Figure 2: Temperature derivative of slowest and fastest TGA run in air. Symbols denote reaction events.

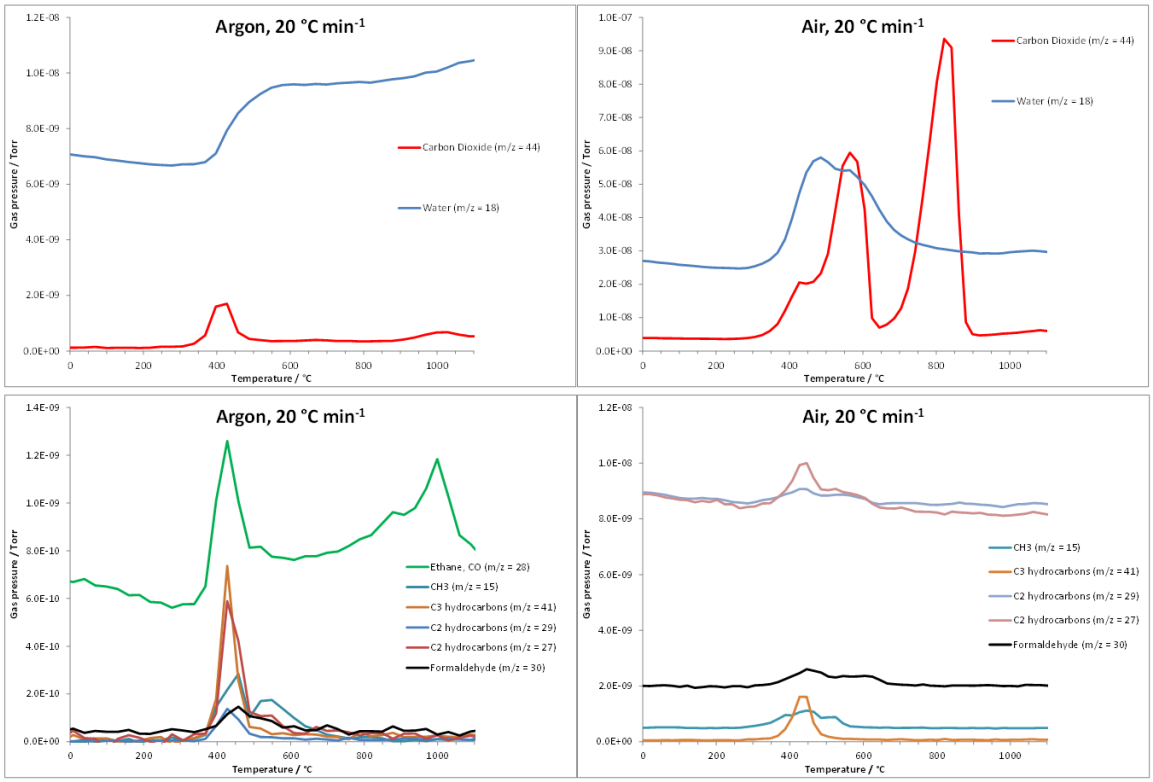

Figure 3: Mass spectrometry response of Technofire® 67152B for the 20 K min^{-1} condition under both argon (left) and air (right).

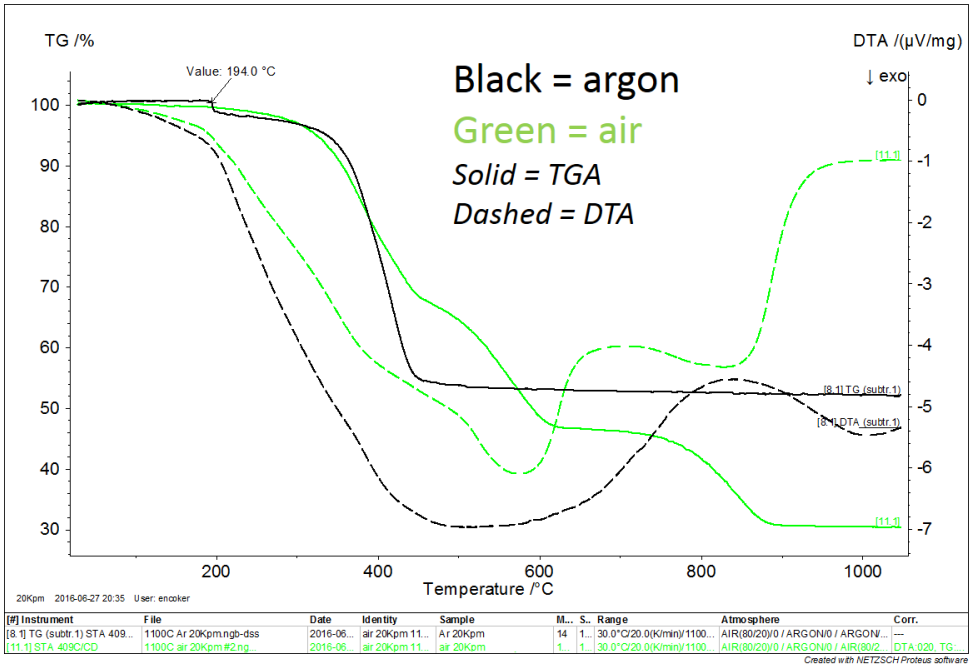

Figure 4: DSC data for Technofire® in air and argon at a ramp rate of 20 K-min^{-1}

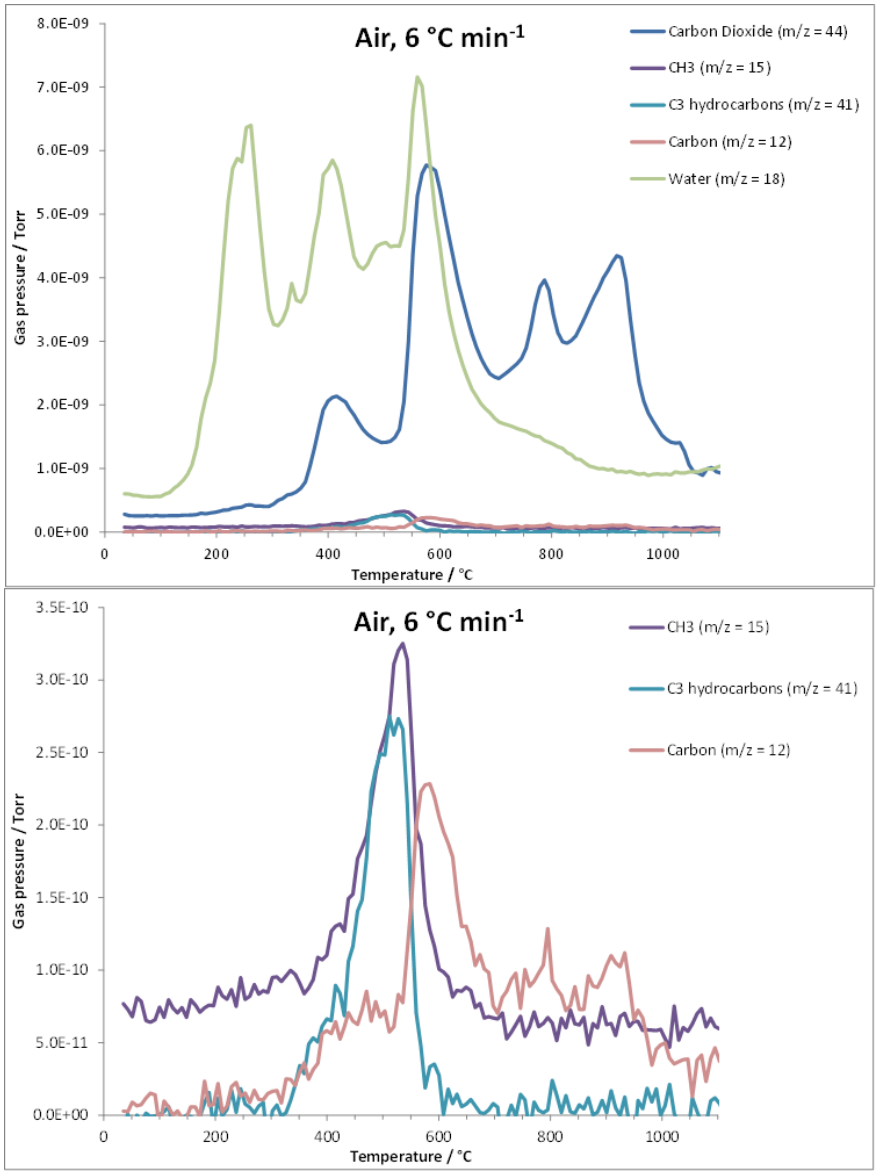

Figure 5: Mass spectrometry response of Pyroclad® X1 for the 6 K min^{-1} condition under an air environment

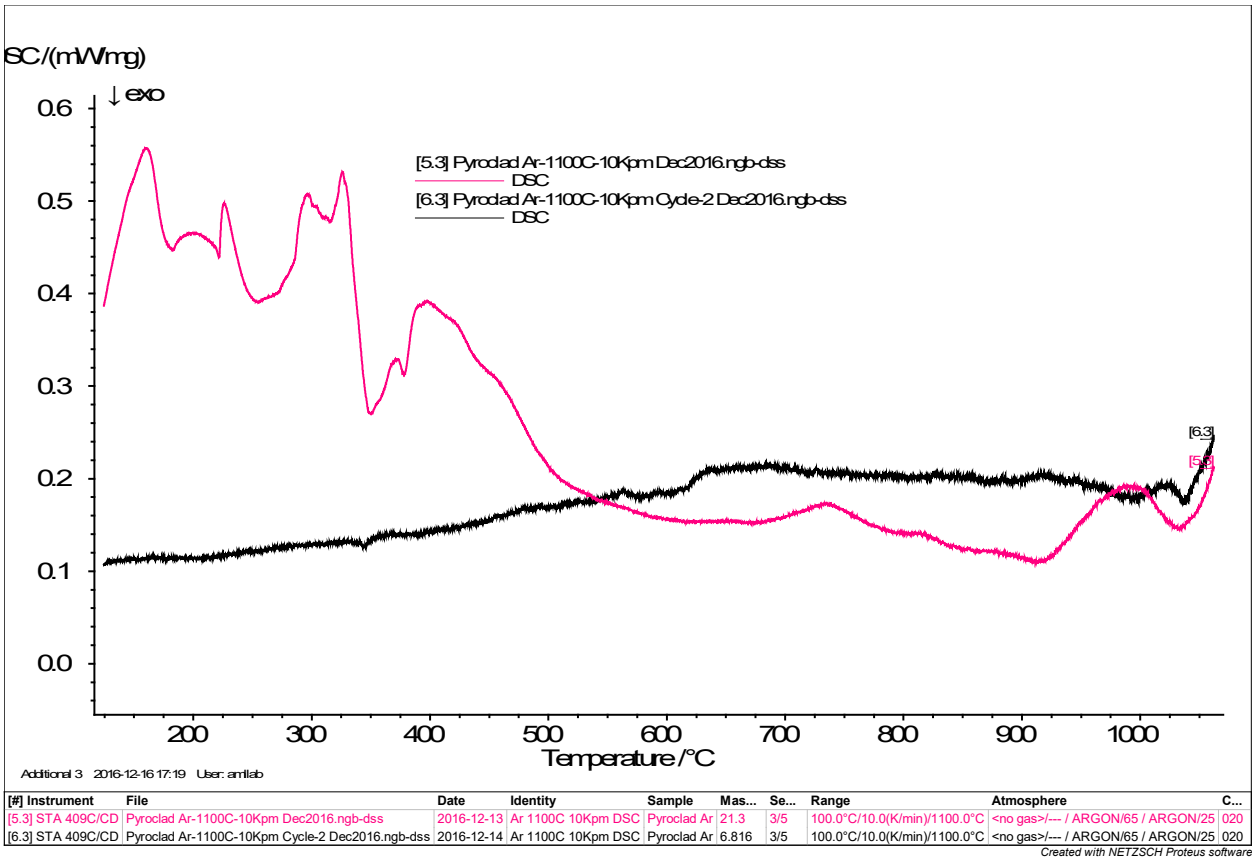

[#] Instrument	File	Date	Identity	Sample	Mas...	Se...	Range	Atmosphere	C...
[5.3] STA 409C/CD	Pyroclad Ar-1100C-10Kpm Dec2016.ngb-dss	2016-12-13	Ar 1100C 10Kpm DSC	Pyroclad Ar	21.3	3/5	100.0°C/10.0(K/min)/1100.0°C	<no gas>/--- / ARGON/65 / ARGON/25	020
[6.3] STA 409C/CD	Pyroclad Ar-1100C-10Kpm Cycle-2 Dec2016.ngb-dss	2016-12-14	Ar 1100C 10Kpm DSC	Pyroclad Ar	6.816	3/5	100.0°C/10.0(K/min)/1100.0°C	<no gas>/--- / ARGON/65 / ARGON/25	020

Created with NETZSCH Proteus software

Figure 6: Differential scanning calorimetry signal for Pyroclad® X1 evaporation/dissociation in Argon

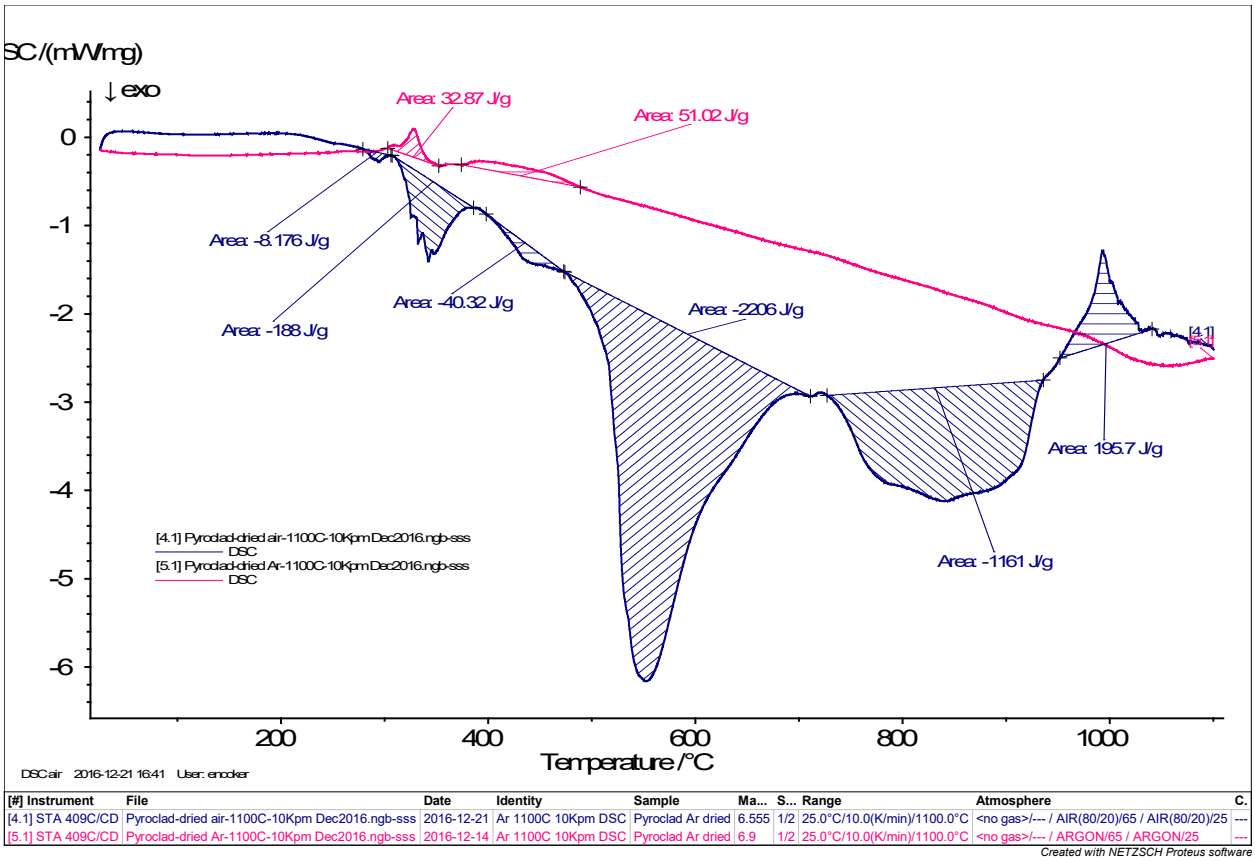

[#]	Instrument	File	Date	Identity	Sample	Ma...	S...	Range	Atmosphere	C.
[4.1]	STA 409C/CD	Pyroclad-dried air-1100C-10Kpm Dec2016.ngb-sss	2016-12-21	Ar 1100C 10Kpm DSC	Pyroclad Ar dried	6.555	1/2	25.0°C/10.0(K/min)/1100.0°C	<no gas>/--- / AIR(80/20)/65 / AIR(80/20)/25	---
[5.1]	STA 409C/CD	Pyroclad-dried Ar-1100C-10Kpm Dec2016.ngb-sss	2016-12-14	Ar 1100C 10Kpm DSC	Pyroclad Ar dried	6.9	1/2	25.0°C/10.0(K/min)/1100.0°C	<no gas>/--- / ARGON/65 / ARGON/25	---

Created with NETZSCH Proteus software

Figure 7: Differential scanning calorimetry signal for pre-dried Pyroclad® X1 in air

3.2. Kinetic Parameter Determination

This study considers four TGA mass time histories for Carboline samples provided by Eric Coker. The tests were conducted at 3, 6, 12, and 20°C/min heating rates with air passing over the samples. It appeared that four reactions should be considered. The simple case of successive condensed states for the remaining material was considered. That is, each state of material reacts to be the sole source of the next material state. Then five condensed materials M_0, M_1, M_2, M_3, and M_4 are involved and each "parent" reacts to form the next material and an unspecified gas, G, which is lost from the system.

$$\text{Reaction 1:} \quad M_0 \rightarrow a_1 M_1 + (1 - a_1) G \tag{2}$$

$$\text{Reaction 2:} \quad M_1 \rightarrow a_2 M_2 + (1 - a_2) G \tag{3}$$

$$\text{Reaction 3:} \quad M_2 \rightarrow a_3 M_3 + (1 - a_3) G \tag{4}$$

$$\text{Reaction 4:} \quad M_3 \rightarrow a_4 M_4 + (1 - a_4) G \tag{5}$$

The four reaction rates are

$$r_i = B_i \exp\left[-\frac{E_i}{RT} \right] \tag{6}$$

for i = 1, 2, 3, and 4. Then five rate equations for appearance/disappearance of the materials are

$$\frac{dM_0}{dt} = -M_0 r_1 \tag{7}$$

$$\frac{dM_1}{dt} = -M_1 r_2 + a_1 M_0 r_1 \tag{8}$$

$$\frac{dM_2}{dt} = -M_2 r_3 + a_2 M_1 r_2 \tag{9}$$

$$\frac{dM_3}{dt} = -M_3 r_4 + a_3 M_2 r_3 \tag{10}$$

$$\frac{dM_4}{dt} = a_4 M_3 r_4 \tag{11}$$

These equations were integrated through time numerically for candidate sets of the model's fixed parameters (a_i, B_i, E_i) giving 12 adjustable parameters for the model. Further constraints were:

$$E_i < E_{i+1} \tag{12}$$

and

$$a_i \leq 1 \tag{13}$$

The constraint indicated by Equation 12 was utilized initially and the result was that the last three reactions all ended up with the same activation energies. While the constraint helped to find parameters putting the solution in the neighborhood of measurements, the result of the middle two reactions being constrained to a lower activation energy seemed unnecessary. Consequently, the

search was run again with the constraint of equation 11 removed. New parameters resulted with the final metric of "goodness-of-fit" (Equation 15) being improved about 0.5%.

At any point in time the system mass is the sum of all the condensed phases, that is:

$$S(t) = \sum_{j=1}^{5} M_j(t) \tag{14}$$

All four heating rates were considered over the time intervals of each experiment, so an objective function was formed:

$$H = \sum_{i=1}^{4} \sum_{j=1}^{N_i} \left[1 - \frac{S(t_j)}{F_i(t_j)} \right]^2 \tag{15}$$

Where $F_i(t_j)$ is the measured mass fraction from the i^{th} experiment. The discrete times from each experiment were the successive times at which 3°C temperature increases occurred in the experimental record. So, there were 330 to 336 time points picked from each of the four experiments along with the corresponding measured temperatures.

A univariate search was used. A golden-section search was used on one variable at a time. The convergence was very slow but steady. The search would nominally step through the parameters with a probability of jumping to some random other parameter.

The result of the search is presented in Table 3:

Table 3: Optimized parameter-search variables

i	a_i	B_i (1/s)	E_i (J/kmol)
1	0.84439	4.04038E2	5.06451E7
2	0.59984	5.00049E8	1.38260E8
3	0.77508	1.33007E5	1.17365E8
4	0.78870	3.13588E2	1.06592E8

Figure 8 is a plot of the four measured (solid lines) and four model-predicted (dashed lines) mass histories for the temperature histories of the four experiments as a function of temperature. Figure 9 is a plot of the four measured (solid lines) and four model-predicted (dashed lines) mass histories for the temperature histories of the four experiments as a function of time. Figure 10 shows the predicted abundance of M_0, M_1, M_2, M_3, and M_4 as a function of time. The heaviest lines are M_0 and line heft diminishes to the thinnest which are M_4. The colors are close to those in the previous two figures with green, blue, purple, and red respectively corresponding to 3, 6, 12, and 20K/min heating rates.

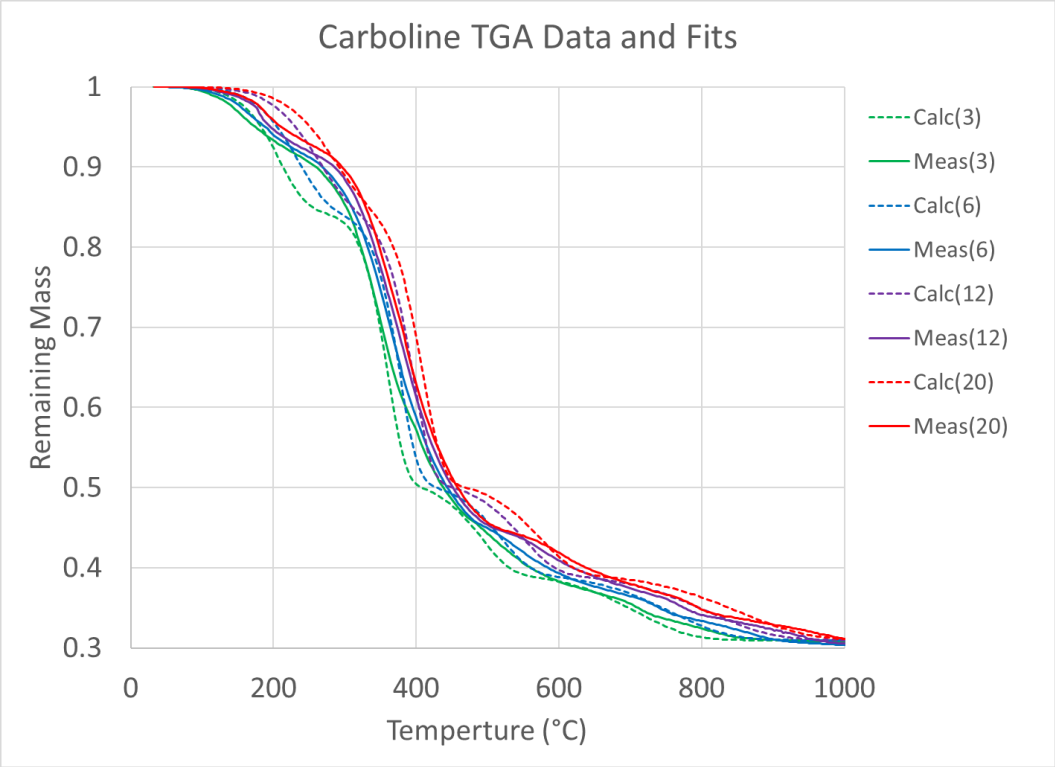

Figure 8: Measured and calculated mass loss curves as a function of temperature for the four experiments.

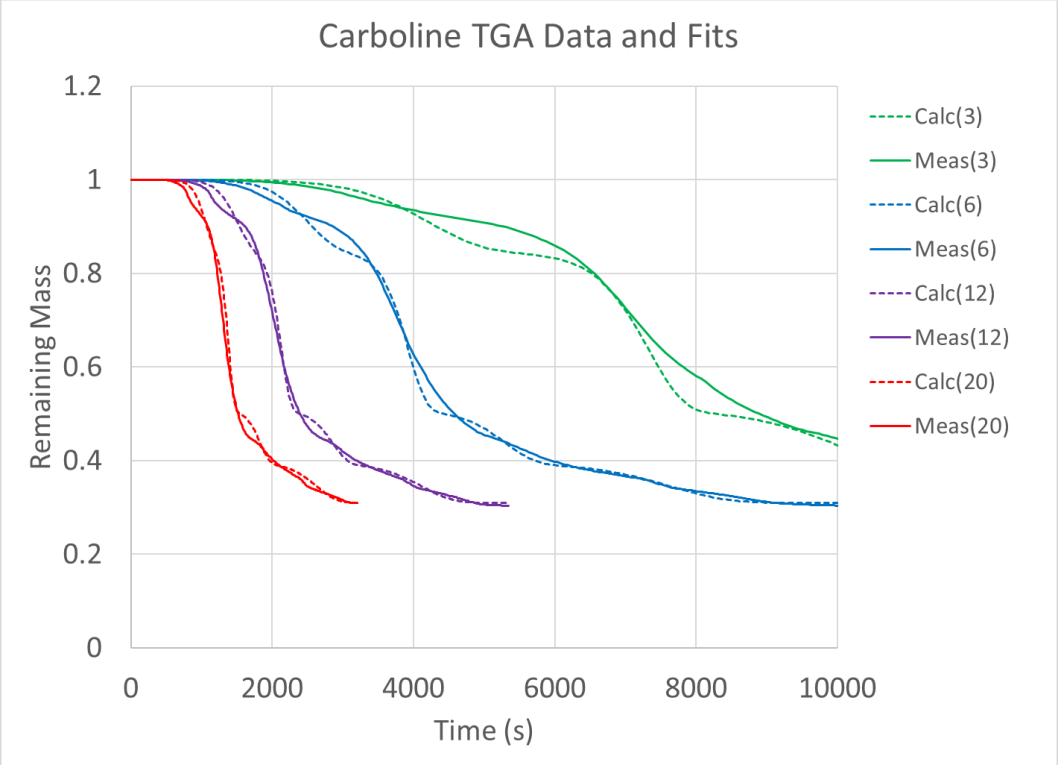

Figure 9: Measured and calculated mass loss curves as a function of time for the four experiments.

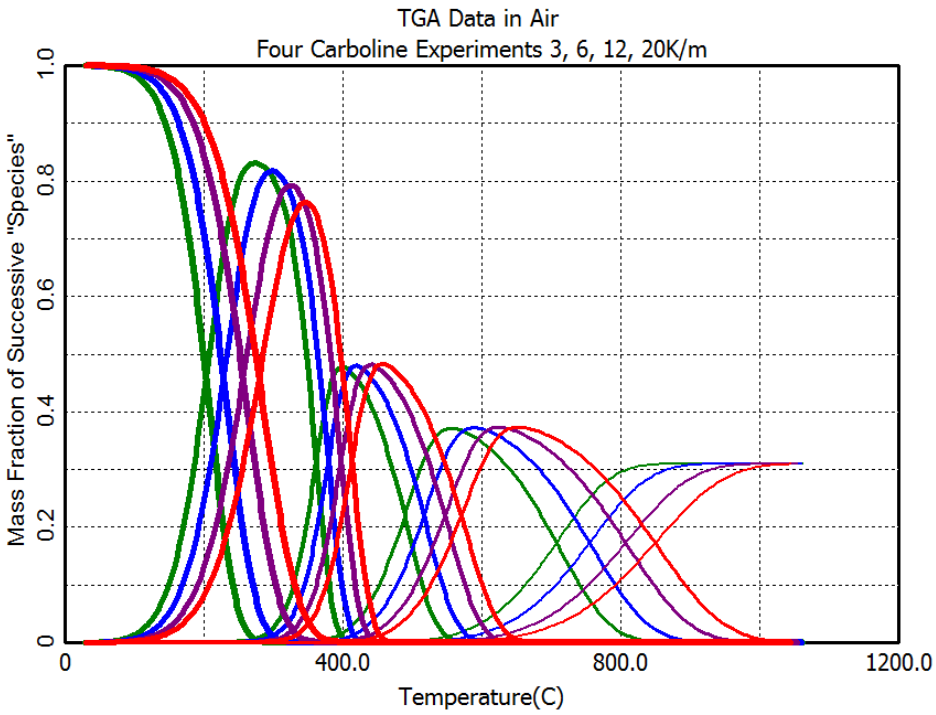

Figure 10: Abundance of each "species" as a function of temperature for the four experiments.

The preceding results are proposed for use as a chemical model to be implemented in CHEMEQ in Aria. Additional interpretation of data taken on small samples is needed to associated energies of reaction with the reactions proposed here.

Two modifications to the reaction equation sets were considered. Equations 2 to 5 and correspondingly 7 to 11 were modified to allow the first reaction (Equations 2 and 2) to produce M_4. This introduced a thirteenth parameter which was a second stoichiometric coefficient on the right-hand side of the reaction. This same modification was considered in which the second reaction (Equations 3 and 8) were allowed to produce M_4. The parameter optimization for either of these adjustments "chose" to produce about 2% M_4 and resulted in less than $1/10{,}000^{th}$ improvement in the goodness-of-fit measure (Equation 15). Consequently, the simplicity of a model with one less parameter was preferred, and these modifications were abandoned.

The comparison shown in Figure 9 is deemed reasonable as basis to attempt to model the heat transfer. The fastest temperature rise condition (20K/min) is likely smaller than the rates of real interest due to threatening environments.

3.3. Generation of ChemEQ reactive material definition in Aria

The relevant parameters extracted from the previous sections for Pyroclad® X1 are included in a ChemEQ materials definition in Aria. ChemEQ allows for Arrhenius-style reaction descriptions to simulate both extent of reaction and energy releases. In this definition, the optimized search parameters from Table 3, as well as the energy releases summarized in Table 1. Parameters not currently accounted for in this document are changes in material density and thermal conductivity

during expansion. These phenomena are accounted for by empirical fits to test data and are implemented through a separate user sub-routine.

```
    BEGIN Aria MATERIAL Pyroclad
      use data block foam_data
      Density = calore_user_sub name = vDensity type = element # kg/m^3
      emissivity = constant e = 1.0
      thermal conductivity = calore_user_sub name = effectiveK type = element
      specific heat = user_function X=Temperature Name = EricsCp
      Heat Conduction = basic

      BEGIN PARAMETERS FOR CHEMEQ MODEL reactModel          number of reactions is 4
         species names are M0 M1 M2 M3 M4 Gas
         species phases are Condensed Condensed Condensed Condensed Condensed Gas
         condensed fraction is 1.                # Not used
         steric coefficients are 0.0 0.0 0.0 0.0
         log preexponential factors are 6.001508933   20.03021665 11.79815704 5.748080022

         activation energies are 5.064510E+07   1.382600E+08   1.173650E+08   1.065920E+08
         energy releases are -2.5408E+08 3.6086652E+07 1.758696E+08 8.8018245E+07

         concentration exponents for  M0 ARE 1.0 0.0  0.0 0.0 # r1 is proportional to M0 present
         concentration exponents for  M1 ARE 0.0 1.0  0.0  0.0  # r2 is proportional to M1
present
         concentration exponents for  M2 ARE 0.0 0.0 1.0  0.0  # r3 is proportional to M2 present
         concentration exponents for  M3 ARE 0.0 0.0 0.0 1.0   # no reaction cares
         concentration exponents for  M4 ARE 0.0 0.0  0.0 0.0  # no reaction cares
         concentration exponents for  Gas ARE 0.0 0.0  0.0 0.0 # no reaction cares

         stoichiometric coefficients for  M0 ARE -1.0 0.0 0.0 0.0          # M0 dA/dt = -r1
         stoichiometric coefficients for  M1 ARE 0.84439 -1.0 0.0   0.0  # M1
         stoichiometric coefficients for  M2 ARE 0.0 0.59984 -1.0   0.0      # M2
         stoichiometric coefficients for  M3 ARE 0.0 0.0 0.77508   -1.0        # M3
         stoichiometric coefficients for  M4 ARE 0.0 0.0 0.0 0.7887       # M4
         stoichiometric coefficients for  Gas ARE 0.15561 0.40016 0.22492 0.2113# Gas

         aux variable names are M0frac, M1frac, M2frac, M3frac, M4frac, gasfrac, sfrac, keff, ER,
absNow
         aux variable subroutine is calcauxvar
       END PARAMETERS FOR CHEMEQ MODEL reactModel
   END Aria MATERIAL Pyroclad
```

3.3.1. Specific Heat

The specific heat as a function of temperature is given as:

```
begin definition for function EricsCp
 type = piecewise linear
 scale by 1.0
begin values
#t Cp
318.671  1194.7
320.671  1225.58
322.671  1250.75
324.671  1269.48
326.671  1288.74
328.671  1302.57
330.671  1317.69
332.671  1343.71
334.671  1356.68
336.671  1373.65
338.671  1385.05
340.671  1402.2
342.671  1414.57
344.671  1430.43
```

```
346.671  1443.01
348.671  1455.92
350.671  1472.26
352.671  1479.9
354.671  1490.66
356.671  1496.89
358.671  1505.69
360.671  1507.23
362.671  1519.18
364.671  1517.74
366.671  1530.73
368.671  1543.51
370.671  1552.1
372.671  1564.08
374.671  1578.46
376.671  1589.21
378.671  1601.46
380.671  1619.28
382.671  1643.29
384.671  1675.94
386.671  1698.16
388.671  1703.22
390.671  1700.7
392.671  1697.1
394.671  1694.77
396.671  1692.22
398.671  1687.48
400.671  1677.21
402.671  1672.41
404.671  1667.51
406.671  1663.15
408.671  1653.51
410.671  1649.24
412.671  1647.13
414.671  1642.45
416.671  1642.27
418.671  1642.79
420.671  1639.35
422.671  1638.42
424.671  1639.26
426.671  1634.73
428.671  1638.55
430.671  1635.73
432.671  1636.12
434.671  1637.76
436.671  1641.03
438.671  1642.67
440.671  1545.51
442.671  1594.23
444.671  1652.61
446.671  1650.98
448.671  1659.24
450.671  1633.23
end values
 end definition for function EricsCp
```

4. CONCLUSIONS

This report serves to document the test results of two intumescent materials: Technical Fibre Products Technofire® 67152B and Carboline Pyroclad® X1. Both materials were characterized through thermogravimetric and differential scanning calorimetry analyses. The preferred material, Carboline Pyroclad® X1, was further characterized to determine the reaction kinetics and reaction enthalpies so as to be modeled in the thermal analysis software Aria. An Aria materials definition is presented using the reactive ChemEq materials definition. This materials definition is currently being used to model the thermal response of geometries featuring this reactive material.

This page left blank

REFERENCES

[1] G. J. Griffin, "The Modeling of Heat Transfer across Intumescent Polymer Coatings," *Journal of Fire Sciences*, vol. 28, no. 3, pp. 249–277, May 2010, doi: 10.1177/0734904109346396.

[2] J. E. J. Staggs, R. J. Crewe, and R. Butler, "A theoretical and experimental investigation of intumescent behaviour in protective coatings for structural steel," *Chemical Engineering Science*, vol. 71, pp. 239–251, Mar. 2012, doi: 10.1016/j.ces.2011.12.010.

[3] C. Di Blasi and C. Branca, "Mathematical model for the nonsteady decomposition of intumescent coatings," *AIChE Journal*, vol. 47, no. 10, pp. 2359–2370, 2001, doi: https://doi.org/10.1002/aic.690471020.

[4] C. Di Blasi, "Modeling the effects of high radiative heat fluxes on intumescent material decomposition," *Journal of Analytical and Applied Pyrolysis*, vol. 71, no. 2, pp. 721–737, Jun. 2004, doi: 10.1016/j.jaap.2003.10.003.

[5] M. Jimenez, S. Duquesne, and S. Bourbigot, "Multiscale Experimental Approach for Developing High-Performance Intumescent Coatings," *Ind. Eng. Chem. Res.*, vol. 45, no. 13, pp. 4500–4508, Jun. 2006, doi: 10.1021/ie060040x.

[6] R. J. Asaro, B. Lattimer, C. Mealy, and G. Steele, "Thermo-physical performance of a fire protective coating for naval ship structures," *Composites Part A: Applied Science and Manufacturing*, vol. 40, no. 1, pp. 11–18, Jan. 2009, doi: 10.1016/j.compositesa.2008.07.015.

[7] A. P. Mouritz, S. Feih, E. Kandare, and A. G. Gibson, "Thermal–mechanical modelling of laminates with fire protection coating," *Composites Part B: Engineering*, vol. 48, pp. 68–78, May 2013, doi: 10.1016/j.compositesb.2012.12.001.

[8] B. K. Kandola, P. Luangtriratana, S. Duquesne, and S. Bourbigot, "The Effects of Thermophysical Properties and Environmental Conditions on Fire Performance of Intumescent Coatings on Glass Fibre-Reinforced Epoxy Composites," *Materials (Basel)*, vol. 8, no. 8, pp. 5216–5237, Aug. 2015, doi: 10.3390/ma8085216.

[9] G. Landucci, M. Molag, J. Reinders, and V. Cozzani, "Experimental and analytical investigation of thermal coating effectiveness for 3m(3) LPG tanks engulfed by fire," *J Hazard Mater*, vol. 161, no. 2–3, pp. 1182–1192, Jan. 2009, doi: 10.1016/j.jhazmat.2008.04.097.

[10] Sean Younger, Dwayne Meyer, and Dallas Finch, "Industrial Fireproofing: Setting the Story Straight," *Materials Performance*, vol. 51, no. 10, Oct. 01, 2012.

[11] A. Bhargava and G. J. Griffin, "A Two Dimensional Model of Heat Transfer Across a Fire Retardant Epoxy Coating Subjected to an Impinging Flame," *Journal of Fire Sciences*, vol. 17, no. 3, pp. 188–208, May 1999, doi: 10.1177/073490419901700304.

[12] C. Branca, C. Di Blasi, and H. Horacek, "Analysis of the Combustion Kinetics and Thermal Behavior of an Intumescent System," *Ind. Eng. Chem. Res.*, vol. 41, no. 9, pp. 2107–2114, May 2002, doi: 10.1021/ie010841u.

[13] *Pyroclad X1 Application Manual*, Rev 3. 2150 Schuetz Rd, St. Louis, MO 63146: Carboline, 2014.

[14] "Pyroclad® X1 Product Data Sheet." Carboline, Oct. 01, 2020.

[15] F. Sevim, F. Demir, M. Bilen, and H. Okur, "Kinetic analysis of thermal decomposition of boric acid from thermogravimetric data," *Korean J. Chem. Eng.*, vol. 23, no. 5, pp. 736–740, Sep. 2006, doi: 10.1007/BF02705920.

DISTRIBUTION

Email—Internal

Name	Org.	Sandia Email Address
Karen Son	1514	knson@sandia.gov
Flint Pierce	1514	fpierce@sandia.gov
Leslie Phinney	1514	lmphinn@sandia.gov
Wyatt Hodges	1514	whodges@sandia.gov
Lorraine Guerin	1514	lcgueri@sandia.gov
Roy Hogan	1514	rehogan@sandia.gov
Nathan Porter	1544	nwporte@sandia.gov
Anay Luketa	1532	aluketa@sandia.gov
Stefan Domino	1541	spdomin@sandia.gov
Blake Reece	6651	bdreece@sandia.gov
Technical Library	1911	sanddocs@sandia.gov

This page left blank

Sandia National Laboratories

Sandia National Laboratories is a multimission laboratory managed and operated by National Technology & Engineering Solutions of Sandia LLC, a wholly owned subsidiary of Honeywell International Inc. for the U.S. Department of Energy's National Nuclear Security Administration under contract DE-NA0003525.